

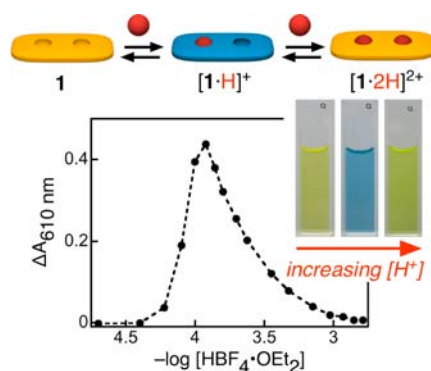
Three-Stage Binary Switching of Azoaromatic Polybase

Ho Yong Lee, András Olasz, Chun-Hsing Chen, and Dongwhan Lee*

Department of Chemistry, Indiana University, 800 East Kirkwood Avenue, Bloomington, Indiana 47405, United States

dongwhan@indiana.edu

Received November 6, 2012

ABSTRACT

An OFF–ON–OFF-type three-stage binary switching was realized with an azoaniline-based polybase **1**. The optical properties of **1** and $[1 \cdot 2H]^{2+}$ are essentially indistinguishable to the naked eye but distinctively different from those of $[1 \cdot H]^+$ to produce an unusual *bell-shaped response* as a function of protonation state; the underlying molecular mechanism was unraveled by a combination of experimental and DFT computational studies.

Carbon-based π -conjugation can be structurally engineered with functional groups that respond to external stimuli. With appropriate structure design, the geometric and/or electronic properties of such hybrid π -systems can be modulated in a predictable and controllable fashion.¹ Azoaromatics represent one important class of such a functional motif,² which have found applications as chemical sensors and switches that exploit either (i) light-driven *trans*–*cis* isomerization around the —N=N— bond for

*mechanical signaling*³ or (ii) binding-induced perturbation of the electronic structure of the extended π -conjugation for *optical signaling*.⁴

In this paper, we report *three-stage binary signaling* of an azopyrrole system **1** (Scheme 1) having multiple Brønsted basic sites embedded along the π -conjugated molecular backbone. Unlike simple ON–OFF or OFF–ON switching (Scheme 1b) of typical receptors/indicators as chemical models of logic operation,⁵ the implementation of three-stage binary switching, such as the OFF–ON–OFF or ON–OFF–ON sequence shown in Scheme 1a requires a structural platform **I** that has *multiple binding sites* for *common substrates* functioning as an input signal. In addition, a stepwise and reversible binding event of **I** should generate discrete and experimentally identifiable adducts,

(1) (a) Balzani, V.; Venturi, M.; Credi, A. *Molecular Devices and Machines: A Journey into the Nanoworld*; Wiley–VCH: Weinheim, 2003. (b) Kay, E. R.; Leigh, D. A.; Zerbetto, F. *Angew. Chem., Int. Ed.* **2007**, *46*, 72–191. (c) de Silva, A. P.; Vance, T. P.; West, M. E. S.; Wright, G. D. *Org. Biomol. Chem.* **2008**, *6*, 2468–2481. (d) Stoddart, J. F. *Chem. Soc. Rev.* **2009**, *38*, 1802–1820. (e) *Molecular Switches*, 2nd ed.; Feringa, B. L., Browne, W. R., Eds.; Wiley–VCH: Weinheim, 2011.

(2) (a) *The Chemistry of the hydrazo, azo and azoxy groups*; Patai, S., Ed.; John Wiley & Sons: London, 1975. (b) Tamai, N.; Miyasaka, H. *Chem. Rev.* **2000**, *100*, 1875–1890. (c) Hamon, F.; Djedaini-Pilard, F.; Barbot, F.; Len, C. *Tetrahedron* **2009**, *65*, 10105–10123. (d) Merino, E. *Chem. Soc. Rev.* **2011**, *40*, 3835–3853. (e) Beharry, A. A.; Woolley, G. A. *Chem. Soc. Rev.* **2011**, *40*, 4422–4437.

(3) (a) Russev, M.-M.; Hecht, S. *Adv. Mater.* **2010**, *22*, 3348–3360. (b) Stoll, R. S.; Hecht, S. *Angew. Chem., Int. Ed.* **2010**, *49*, 5054–5075. (c) Yu, H.; Ikeda, T. *Adv. Mater.* **2011**, *23*, 2149–2180. (d) Wegner, H. A. *Angew. Chem., Int. Ed.* **2012**, *51*, 4787–4788.

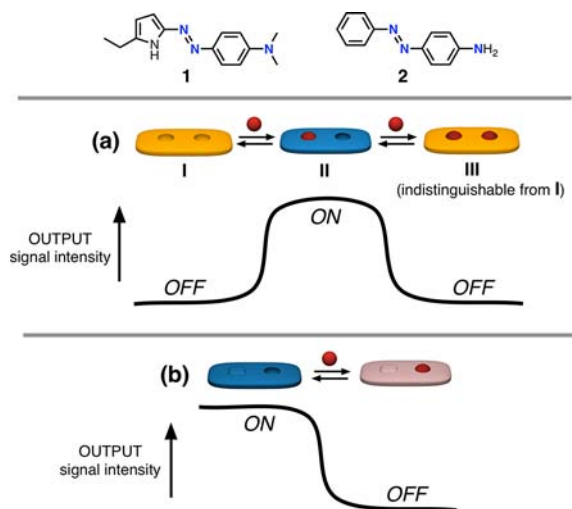
(4) (a) Zollinger, H. *Color Chemistry: Syntheses, Properties, and Applications of Organic Dyes and Pigments*, 3rd ed.; VCH: Zurich, 2003. (b) Chudgar, R. J.; Oakes, J. In *Kirk-Othmer Encyclopedia of Chemical Technology*, 5th ed.; John Wiley & Sons: Hoboken, 2007; Vol. 9, pp 349–430.

(5) (a) de Silva, A. P.; Uchiyama, S. *Nat. Nanotechnol.* **2007**, *2*, 399–410. (b) Szacilowski, K. *Chem. Rev.* **2008**, *108*, 3481–3548. (c) Andréasson, J.; Pischel, U. *Chem. Soc. Rev.* **2010**, *39*, 174–188.

II and **III** (Scheme 1a). Most importantly, the signal output from the “fully-saturated” product **III** should be distinctively different from that of the “intermediate” **II**, but *operationally indistinguishable* from that of the initial state **I**, so that a bell-shaped response curve (Scheme 1a) is obtained with an increasing level of input signal.

When all these functional requirements are satisfied, the **ON** signal from such a system is observed only for a finite input signal window that maximizes the population of **II**. By design, the system automatically turns **OFF** when the input signal level is either lowered (toward **I**) or raised (toward **III**) away from this predefined zone of **II**. A fluorogenic polybase reported by de Silva is a seminal example of such a molecular switch,⁶ which uses protons as an input signal to produce a bell-shaped response curve (Scheme 1a) resulting from pH-dependent PET mechanisms.^{1c,7}

Scheme 1. Chemical Structures of **1** and **2** (top), and Schematic Representations of (a) Three-Stage vs (b) Two-Stage Binary Switching upon Substrate (Shown As a Red Sphere) Binding



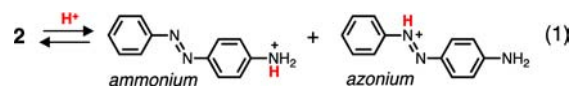
Our entry into this chemistry was motivated by **2** (Scheme 1), a prototypical azoaniline that we came across during our studies of electron-rich azo derivatives for chemical sensing and actuation.⁸ As a simpler structural

(6) de Silva, A. P.; Gunaratne, H. Q. N.; McCoy, C. P. *Chem. Commun.* **1996**, 2399–2400.

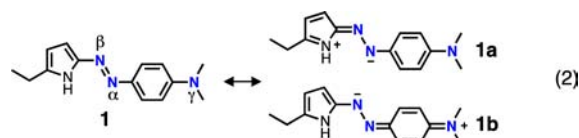
(7) For conceptually related luminescence-based **OFF–ON–OFF** signaling systems responding to protons, see: (a) Fabbrizzi, L.; Gatti, F.; Pallavicini, P.; Parodi, L. *New J. Chem.* **1998**, 22, 1403–1407. (b) Gunnlaugsson, T.; Leonard, J. P.; Sénéchal, K.; Harte, A. J. *J. Am. Chem. Soc.* **2003**, 125, 12062–12063. (c) Han, M.-J.; Gao, L.-H.; Lü, Y.-Y.; Wang, K.-Z. *J. Phys. Chem. B* **2006**, 110, 2364–2371. (d) Evangelio, E.; Hernando, J.; Imaz, I.; Bardají, G. G.; Alibés, R.; Busqué, F.; Ruiz-Molina, D. *Chem.—Eur. J.* **2008**, 14, 9754–9763. (e) Pais, V. F.; Remón, P.; Collado, D.; Andréasson, J.; Pérez-Inestrosa, E.; Pischel, U. *Org. Lett.* **2011**, 13, 5572–5575. (f) Chen, Y.; Wang, H.; Wan, L.; Bian, Y.; Jiang, J. *J. Org. Chem.* **2011**, 76, 3774–3781. (g) Sadhu, K. K.; Mizukami, S.; Yoshimura, A.; Kikuchi, K. *Org. Biomol. Chem.* **2013**, in press (DOI: 10.1039/C2OB26630J).

(8) (a) Lee, H. Y.; Song, X.; Park, H.; Baik, M.-H.; Lee, D. *J. Am. Chem. Soc.* **2010**, 132, 12133–12144. (b) Lee, H. Y.; Jo, J.; Park, H.; Lee, D. *Chem. Commun.* **2011**, 47, 5515–5517. (c) Jo, J.; Lee, H. Y.; Liu, W.; Olsz, A.; Chen, C.-H.; Lee, D. *J. Am. Chem. Soc.* **2012**, 134, 16000–16007.

analogue of pH indicator methyl yellow or methyl orange, **2** has a *p*-phenylene linker which supports three Brønsted basic nitrogen atoms constituting the extended π -conjugation. Previous studies have shown that its protonation product $[2 \cdot H]^+$ exists as a tautomeric mixture of “ammonium” and “azonium” species (eq 1).⁹



Using **2** as a structural template, we designed **1**.¹⁰ We anticipated that the Brønsted basicity of *both* of the azo nitrogen atoms, $N\alpha$ and $N\beta$, in **1** should be enhanced through contributions from the quinoid-type and zwitterionic resonance structures **1a** and **1b** (eq 2).



In CH_3CN at $T = 298$ K, **1** displayed an intense yellow color, but immediately turned blue upon protonation (Figure 1a, inset). Such behavior was not unusual for an azo dye that functions as a simple acid–base indicator. To our surprise, however, subsequent addition of an increasing amount of acid *restored* the initial yellow color, which was visually similar to the neutral **1** (Figure 1a, inset).¹¹ This serendipitous finding of a rather peculiar protonation-dependent color switching did not make any intuitive sense and invited a detailed investigation.

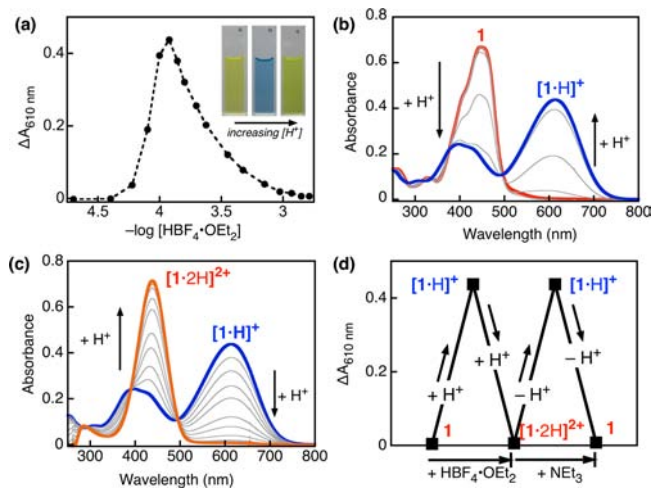


Figure 1. (a) A plot of $\Delta A_{610 \text{ nm}}$ vs $-\log[HBF_4 \cdot OEt_2]$, and yellow–blue–yellow color switching of **1** (inset: photographic images). (b) UV–vis spectra of **1** in the presence of $[HBF_4 \cdot OEt_2] = 0$ (orange), 0.02, 0.04, 0.06, 0.08, 0.10, and 0.12 (blue) mM. (c) UV–vis spectra of **1** in the presence of $[HBF_4 \cdot OEt_2] = 0.12$ (blue), 0.16, 0.20, 0.24, 0.35, 0.47, 0.70, 0.94, 1.20, 1.40, and 1.60 (orange) mM. (d) A reversible color switching monitored by $\Delta A_{610 \text{ nm}}$ after addition of $HBF_4 \cdot OEt_2$ and back-titration with Et_3N . For all measurements, $[1] = 20 \mu M$ in MeCN; $T = 298$ K.

As shown in Figure 1b, the absorption band of **1** at $\lambda_{\max} = 445$ nm initially lost its intensity with increasing $[\text{H}^+]$, with concomitant buildup of a broad longer-wavelength transition at $\lambda_{\max} = 615$ nm along with a blue-shifted feature at $\lambda_{\max} = 400$ nm. This yellow-to-blue color change, however, was essentially reversed upon further addition of acid (Figure 1c), which elicited the evolution of a new absorption band at $\lambda_{\max} = 440$ nm and complete disappearance of the features at $\lambda_{\max} = 615$ and 400 nm. Such protonation-driven spectral changes can be tracked best by a plot of ΔA_{610} (= changes in the absorption at $\lambda = 610$ nm) vs $-\log[\text{H}^+]$ (Figure 1a), which produces an **OFF–ON–OFF** response function (Scheme 1) with genuine reversibility in the forward (= protonation) and backward (= deprotonation) scans (Figure 1d).

In order to investigate the structural basis of this unusual color switching, we carried out ^1H NMR titration studies. As shown in Figure 2, protonation of **1** with $\text{HBF}_4 \cdot \text{OEt}_2$ in CD_3CN resulted in systematic downfield shifts of the signals from the phenyl protons that are *ortho* to the amine $\text{N}\gamma$ position. This spectral change is also accompanied by downfield shifts in the two pyrrolic C–H resonances.

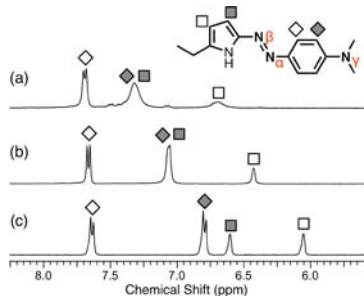
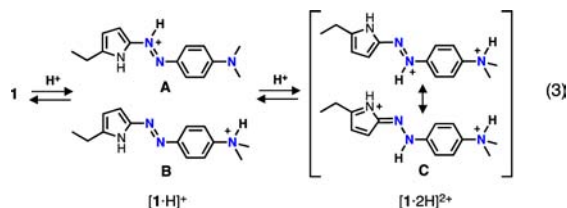


Figure 2. Partial ^1H NMR spectra of **1** (16 mM) in CD_3CN in the presence of (a) 2, (b) 1, and (c) 0 equiv of $\text{HBF}_4 \cdot \text{OEt}_2$ ($T = 298$ K).

In contrast, the phenyl C–H protons that are *ortho* to the azo $\text{N}\alpha$ site remain essentially invariant under this condition. This observation suggests the solution equilibrium described by eq 3; protonation of **1** occurs at its $\text{N}\beta$ or $\text{N}\gamma$ position to furnish a mixture of **A** and **B**. This interpretation is consistent with findings made for the benchmark system **2** (eq 1).⁹

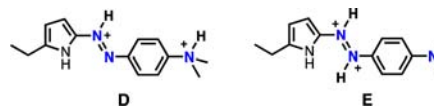


Our subsequent DFT computational studies have confirmed that **A** and **B** share an essentially identical

(9) (a) Kuroda, Y.; Lee, H.; Kuwae, A. *J. Phys. Chem.* **1980**, *84*, 3417–3423. (b) Liwo, A.; Tempczyk, A.; Widernik, T.; Klentak, T.; Czerminski, J. *J. Chem. Soc., Perkin Trans. 2* **1994**, 71–75. (c) Yatsenko, A. V.; Chernyshev, V. V.; Kurbakov, A. I.; Schenk, H. *Acta Crystallogr.* **2000**, *C56*, 892–894. (d) Matazo, D.; Ando, R.; Borin, A.; Santos, P. *J. Phys. Chem. A* **2008**, *112*, 4437–4443.

conformation, in which the pyrrolic N–H group makes a hydrogen bond with the azo $\text{N}\alpha$ atom ($d_{\text{N}\dots\text{N}} = 2.824$ Å for **A**; 2.707 Å for **B**) to attenuate its basicity. On the other hand, contribution of the resonance structure **1b** (eq 2) enhances the basicity of the $\text{N}\beta$ position to furnish **A**.

Upon addition of a second equivalent of proton, a single adduct **C** emerges as the lowest-energy tautomer of $[\mathbf{1}\cdot 2\text{H}]^{2+}$ (eq 3). Our DFT calculations suggested that alternative isomers **D** and **E** (shown below) would be significantly higher in energy, by ca. 11 and 22 kcal mol^{−1}, respectively, relative to **C**. Apparently, **C** benefits from charge delocalization through resonance (eq 3), which is not allowed for **D**. Adjacent positive charges make **E** the most unlikely tautomer.



From the electronic structure point of view, the singly protonated **A** has its (i) HOMO residing at the electron-rich amino group and the pyrrole π -system and (ii) LUMO dominated by the azo π^* orbital in the middle (Figure 3b).

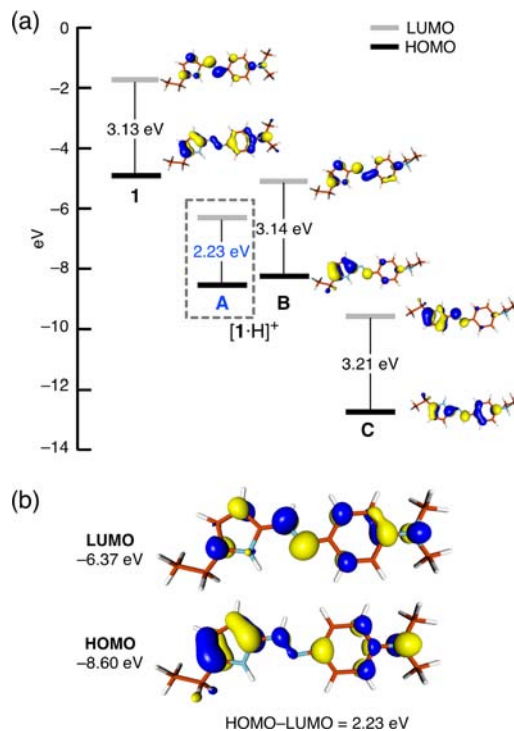


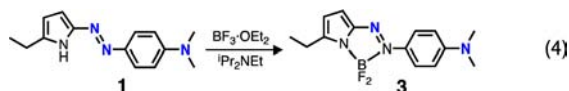
Figure 3. (a) Energy level diagram and FMO isosurface plots. (b) FMO isosurface plots of **A**.

As a consequence, protonation at the $\text{N}\beta$ position results in a smaller HOMO–LUMO gap (2.23 eV) of **A** and promotes longer-wavelength electronic transitions with significant charge-transfer character (Figure 1b). On the other hand, the HOMO–LUMO gap of **B** (3.14 eV) is essentially identical to that (3.13 eV) of

1 (Figures 3a and S1). The intense blue color of $[\mathbf{1}\cdot\text{H}]^+$ thus arises from **A**.

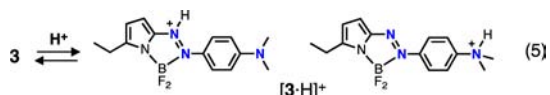
In the doubly protonated **C**, the amine N_γ site is effectively decoupled from the π -conjugation (Figure 3a and S1). The increased HOMO–LUMO gap of **C** (3.21 eV) happens to be close to that (3.13 eV) of **1**, which fully explains their indistinguishable yellow color despite markedly different protonation states (Figure 1a, inset).

The Brønsted acid–base chemistry of **1** is significantly simplified in its derivative **3** (eq 4), in which protonation at the N_α site is effectively blocked through borylation.^{10,12}



The X-ray structure of **3** (Figure 4a) revealed a significant contribution of the quinoid-type resonance structure, as reflected on the C–C bond length alternation in the phenyl ring (C–C = 1.405(1), 1.382(1), 1.417(1), 1.419(1), 1.376(1), and 1.401(1) Å) and the relatively long N–N distance (1.310(1) Å). This geometric property is reminiscent of **A** (= $[\mathbf{1}\cdot\text{H}]^+$) having similar resonance structures (Figure 4a). Indeed, **3** in MeCN displays an intense blue color with a broad absorption centered at $\lambda_{\text{max}} = 600$ nm (Figure 4b), which “mimics” the optical properties of **A** (Figure 1b).

In a manner similar to the conversion of $[\mathbf{1}\cdot\text{H}]^+$ to $[\mathbf{1}\cdot 2\text{H}]^{2+}$ (Figure 1c), protonation of **3** resulted in the disappearance of the longer-wavelength absorption with concomitant development of a new absorption at $\lambda_{\text{max}} = 500$ nm (Figure 4b). This spectral shift is accompanied by the change in color from blue to pink (Figure 4b, inset). Unlike the situation in **1**, coordination of the Lewis acidic $\{\text{BF}_2\}^+$ fragment disqualifies the N_α position from functioning as a Brønsted base. Consequently, protonation can occur only at the N_γ or N_β position (Figure S2) to drive a conventional two-stage switching (eq 5; Scheme 1b).



In summary, two different dye molecules **1** and **3** were prepared which share a common azopyrrole platform. The stepwise protonation of **1** elicits differential shifts in the

(10) A structurally analogous azopyrrole was investigated previously as a synthetic precursor to NIR-absorbing molecules: Li, Y.; Patrick, B. O.; Dolphin, D. *J. Org. Chem.* **2009**, *74*, 5237–5243.

(11) In strongly acidic solvent (95% H_2SO_4), **2** shows similar color switching behavior.^{9a}

(12) Coordination of $\{\text{BF}_2\}^+$ can also lower the energy of the azo $\pi\text{--}\pi^*$ transition. With appropriate structure design, the *trans*-to-*cis* photoisomerization can be driven by visible light. See: Yang, Y.; Hughes, R. P.; Aprahamian, I. *J. Am. Chem. Soc.* **2012**, *134*, 15221–15224.

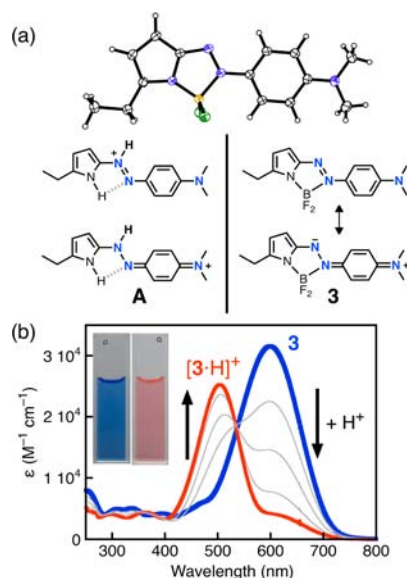


Figure 4. (a) X-ray structure of **3** with thermal ellipsoids at 50% probability (top), and benzoid vs quinoid resonance structures of **A** and **3** (bottom). (b) UV–vis spectra of **3** (20 μM in CH_3CN) in the presence of $[\text{HBF}_4\cdot\text{OEt}_2] = 0$ (blue), 0.20, 0.22, 0.24, and 0.27 (red) mM (inset: photographic images). $T = 298$ K.

HOMO–LUMO gap of the conjugate acid to produce a bell-shaped response of **OFF–ON–OFF** type switching. A dynamic response to the stimuli in *both* directions from the predefined proton concentration window is a defining feature of the three-stage switch **1**, which distinguishes it from the conventional **ON–OFF** system such as **3**. The operation of the three-stage binary switching of **1** capitalizes on the presence of multiple Brønsted basic sites that communicate through the π -conjugation to modulate the energy levels of the frontier MOs as a function of protonation level. Efforts are currently underway in our laboratory to generalize this concept and structurally elaborate this proof-of-concept system for applications in chemical sensing.

Acknowledgment. We thank DTRA/Army Research Office (W911NF-07-1-0533) for financial support of this work.

Supporting Information Available. Experimental procedures, and spectroscopic, X-ray crystallographic, and computational data. This material is available free of charge via the Internet at <http://pubs.acs.org>.

The authors declare no competing financial interest.